Proceedings of the
International Conference on Mechanical Engineering 2009
(ICME2009) 26- 28 December 2009, Dhaka, Bangladesh

ICME09-AM-10

VIBRATION CONTROL OF SMART COMPOSITE SHELL STRUCTURES USING GENETIC ALGORITHM

Debabrata Chakraborty[1] **and Tarapada Roy**[2]

[1]Mechanical Engineering, IIT Guwahati, India
[2]Mechanical Engineering, NIT Rourkela, Orissa, India

ABSTRACT

The present article deals with the optimal vibration control of smart fiber reinforced polymer (FRP) composite structures using layered shell finite element and linear quadratic regulator (LQR) optimal control scheme. Coupled electromechanical finite element (FE) formulations have been developed for analysis of smart curved shell structures having piezoelectric sensors and actuators patches. A real coded GA based LQR control scheme has been used for designing an optimal controller to maximize closed loop damping ratio while keeping actuation voltage within the limit. The developed GA based LQR control has been applied to smart FRP ellipsoidal composite shells structures for simulation of active vibration control. It has been observed that the present GA based design of smart structures for determination of optimal control gain is far superior to the conventional design using LQR in terms of effective closed loop damping ratio.

Keywords: Smart Structures, Active Control, Genetic Algorithm.

1. INTRODUCTION

Most of the lightweight FRP structures are susceptible to large vibration with long decay time and thus require suitable integration of active control means to show better performance under operation. Piezoelectric materials integrated with such structures can act as sensors and actuators thus making the structure smart. This kind of smart structures could be used for active vibration control. At present, the linear quadratic regulator (LQR) control approach has been extensively used in vibration control with appropriate weighting matrices, which gives optimal control-gain by minimizing the performance index. Even though, trial and error method is used to select the weighting matrices, an optimal selection of weighting matrices is of significant importance from the control point of view. Some of the important works in this direction are presented in the following paragraph.

Bhattacharya et al [1] used linear quadratic regulator (LQR) strategy for vibration suppression of spherical shells made of laminated composites by trial and error selection of [Q] and [R] matrices. Ang et al [2] proposed the use of total weighted energy method to select the weighting matrices. Narayanan and Balamurugan [3] presented finite element modeling of laminated structures with distributed piezoelectric sensor and actuator layers and applied LQR control scheme to control the displacement by trial and error selection of [Q] and [R] matrices. In recent years, genetic algorithm (GA) has been extensively applied for optimization of engineering problems and some of the important works on application of GA are described here. Binary coded GA has been applied by Han and Lee [4] to find locations of two piezoelectric sensors and actuators in a cantilever composite plate based on the open loop performance. Sadri et al [5] used Gray coded GA to find the eight coordinates of two piezoelectric actuators in a simply supported plate based on the open loop performance. Abdullah et al [6] used GA to simultaneously place collocated sensor/actuator pairs in multi-storey building while using output feedback as the control law in terms of minimizing the quadratic performance i.e. weighted energy of the system and concluded that the decision variables in this optimization problem were greatly dependent on the selection of weighting matrices [Q] and [R]. Robandi et al [7] presented the use of genetic algorithm for optimal feedback control in multi-machine power system. Deb and Gulati [8] presented simulated binary crossover (SBX) and parameter based mutation operator to be used for effective creation of children solutions from parent solutions. Yang and Soh [9] presented a simultaneous optimization method considering several design variables such as placement of collocated piezoelectric sensors/actuators and size of sensor/actuator and feedback control gain for vibration suppression of simply supported beam by minimizing the equivalent total mechanical energy of the system. However, they did not consider input energy in the used objective function i.e. equivalent total mechanical energy as such did not show the actuators voltages. Wang et al [10] addressed the topology optimization of collocated sensors/ actuators pairs for torsional vibration control of a laminated composite cantilever plate using output feedback control. Liu et al [11] used a spatial H2 norm of

the closed loop transfer matrix for finding the optimal nodal points for sensing displacement and applying actuation for the control of a fixed-fixed plate. Swann and Chattopadhyay [12] developed an optimization procedure to detect arbitrarily located discrete delamination in composite plates using distributed piezoelectric sensors.

From the literature review, it has been observed that a number of works have been reported on the vibration control of simple beam or plate structures.. Most of the published work in this direction used LQR control scheme where [Q] and [R] matrices have been chosen by trial and error, however choice of [Q] and [R] decides the optimal gain. Very few works discussed about actuation voltage while maximizing control performance. Keeping in mind the above points, the present work aims at developing a vibration control module of smart shell structures where the optimal controller will be designed based on a GA-LQR scheme, so that input /actuation voltage is kept within limit.

2. FE FORMULATION AND LQR CONTROL

Figure 1 shows a smart laminated structure having two thin patches of piezoelectric material bonded on the top and bottom surfaces of the base structure. The control laws determine the feedback signal to be given to the actuator depending upon the sensor signal. In Fig.1, *F(t)* is the excited force, ϕ_s is the voltage generated by the sensor and ϕ_a is the voltage input to the actuator in order to control the displacement by developing effective control force.

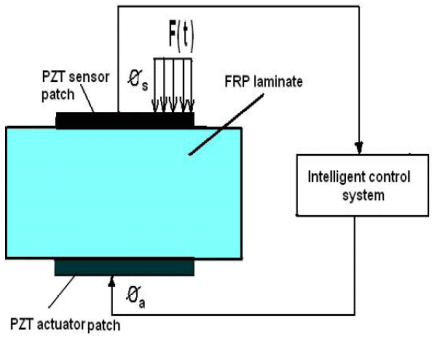

Fig 1. Schematic of a smart laminated plate

In the present formulation, the degenerate shell element [13] kinematics has been considered using a first-order shear deformation theory based on the Reissner–Mindlin assumptions. Figure 2 shows the general smart shell element with composite and piezoelectric layers. It has been assumed that the thin piezoelectric patches are perfectly bonded to the surface of the structure.

In the isoparametric formulation, the coordinates of a point within an element are obtained as

$$\begin{Bmatrix} x \\ y \\ z \end{Bmatrix} = \sum_{k=1}^{8} N_k(\xi,\eta) \begin{Bmatrix} x_k \\ y_k \\ z_k \end{Bmatrix}_{mid} + \sum_{k=1}^{8} N_k(\xi,\eta) \frac{h_k}{2} \zeta V_{3k} \qquad (1)$$

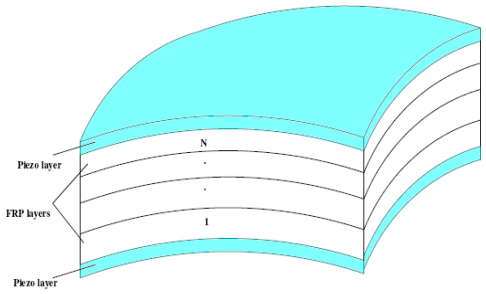

Fig 2. Smart layered shell element.

where $\begin{Bmatrix} x_k \\ y_k \\ z_k \end{Bmatrix}_{mid} = \frac{1}{2}\left(\begin{Bmatrix} x_k \\ y_k \\ z_k \end{Bmatrix}_{top} + \begin{Bmatrix} x_k \\ y_k \\ z_k \end{Bmatrix}_{bottom} \right)$ and h_k is the shell thickness at the node *k*.

The displacement field is described by the five degrees of freedom of a normal viz. the three displacements of its mid-point $\left(u_k \quad v_k \quad w_k\right)^T_{mid}$ and two rotations $\left(\beta_{1k}, \beta_{2k}\right)$. The displacements of a point on the normal resulting from the two rotations are calculated as

$$\begin{Bmatrix} u \\ v \\ w \end{Bmatrix} = \sum_{k=1}^{8} N_k \begin{Bmatrix} u_k \\ v_k \\ w_k \end{Bmatrix}_{mid} + \sum_{k=1}^{8} N_k \zeta \frac{h_k}{2} \begin{bmatrix} V_{1k}^x & -V_{2k}^x \\ V_{1k}^y & -V_{2k}^y \\ V_{1k}^z & -V_{2k}^z \end{bmatrix} \begin{Bmatrix} \beta_{1k} \\ \beta_{2k} \end{Bmatrix} \qquad (2)$$

where u_k, v_k, w_k are the displacements of node *k* on the mid-surface along the global directions respectively, and N_K is the shape function at k^{th} node. Neglecting normal strain component in the thickness direction, the five strain components in the local coordinate system are given by

$$\left[\varepsilon\right] = \begin{bmatrix} \varepsilon_{x'} \\ \varepsilon_{y'} \\ \gamma_{x'y'} \\ \gamma_{x'z'} \\ \gamma_{y'z'} \end{bmatrix} = \begin{bmatrix} \frac{\partial u'}{\partial x'} \\ \frac{\partial v'}{\partial y'} \\ \frac{\partial u'}{\partial y'} + \frac{\partial v'}{\partial x'} \\ \frac{\partial u'}{\partial z'} + \frac{\partial w'}{\partial x'} \\ \frac{\partial v'}{\partial z'} + \frac{\partial w'}{\partial y'} \end{bmatrix} \qquad (3)$$

If $\left\{d_k^e\right\}=\left\{u_k \quad v_k \quad w_k \quad \beta_{1k} \quad \beta_{2k}\right\}^T$ is the vector of nodal variables corresponding to k^{th} node of the element, the generalized nodal variables of an element $\left\{d^e\right\}$ is expresses as $\left\{d^e\right\}=\left\{\left\{d_1^e\right\}^T \quad \left\{d_2^e\right\}^T \quad \left\{d_3^e\right\}^T \quad \left\{d_4^e\right\}^T \quad \left\{d_5^e\right\}^T \quad \left\{d_6^e\right\}^T \quad \left\{d_7^e\right\}^T \quad \left\{d_8^e\right\}^T\right\}$ The strain displacement equation relating the strain components $\{\varepsilon\}$ in global coordinate system to the nodal variables $\{d^e\}$ is expressed as

$$\{\varepsilon\} = \sum_{k=1}^{8} \left[\left(B_u\right)_k^e\right]\left\{d_k^e\right\} = \left[B_u^e\right]\left\{d^e\right\} \qquad (4)$$

and the stress-strain relation in the global coordinate system is

$$\{\sigma\}=[C]\{\varepsilon\} \qquad (5)$$

where $\{\sigma\}=\left[\sigma_x \quad \sigma_y \quad \tau_{xy} \quad \tau_{xz} \quad \tau_{yz}\right]^T$ are the stress components and $[C]$ is the elastic constitutive matrix in global

coordinate system.

The linear piezoelectric constitutive equations coupling the elastic and electric fields can be respectively expressed as the direct and converse piezoelectric equations as

$$\{D\}=[e]\{\varepsilon\}+[\epsilon]\{E\} \tag{6}$$

$$\{\sigma\}=[C]\{\varepsilon\}-[e]^T\{E\} \tag{7}$$

where $\{D\}$ denotes the electric displacement vector, $\{\sigma\}$ denotes the stress vector, $\{\varepsilon\}$ denotes the strain vector and $\{E\}$ denotes the electric field vector. Further $[e]=[d][C]$, where $[e]$ comprises the piezoelectric coupling constants, $[d]$ denotes the piezoelectric constant matrix and $[\epsilon]$ denotes the dielectric constant matrix. The element has been assumed with one electrical degree of freedom at the top of the piezoelectric actuator and sensor patches, ϕ_a^e and ϕ_s^e respectively. Electrical potential has been assumed to be constant over an element and vary linearly through the thickness of piezoelectric patch. For a thin piezoelectric patch, the component of the electric field in the thickness direction is dominant. Therefore, the electric field can be accurately approximated with a non-zero component only in the thickness direction. With this approximation, the electric field strengths of an element in terms of the electrical potential for the actuator and the sensor patches respectively are expressed as

$$\left\{-E_a^e\right\}=\left[B_a^e\right]\left\{\phi_a^e\right\}=\begin{bmatrix}0\\0\\1/h_a\end{bmatrix}\left\{\phi_a^e\right\} \tag{8}$$

$$\left\{-E_s^e\right\}=\left[B_s^e\right]\left\{\phi_s^e\right\}=\begin{bmatrix}0\\0\\1/h_s\end{bmatrix}\left\{\phi_s^e\right\} \tag{9}$$

where subscripts *a* and *s* refer to the actuator patch and the sensor patch, respectively. The superscript *e* denotes the parameter at the element level. $\left[B_a^e\right]$ and $\left[B_s^e\right]$ are the electric field gradient matrices of the actuator and the sensor elements respectively. It should be noted that the electric potential is introduced as an additional degree of freedom on an element level.

The coupled finite element matrix equation derived for a one-element model becomes

$$\begin{pmatrix}\left[M_{uu}^e\right] & [0] & [0]\\ [0] & [0] & [0]\\ [0] & [0] & [0]\end{pmatrix}\begin{Bmatrix}\{\ddot{d}\}\\ \{\ddot{\phi}_a\}\\ \{\ddot{\phi}_s\}\end{Bmatrix}+\begin{pmatrix}\left[K_{uu}^e\right] & \left[K_{ua}^e\right] & \left[K_{us}^e\right]\\ \left[K_{au}^e\right] & \left[K_{aa}^e\right] & [0]\\ \left[K_{su}^e\right] & [0] & \left[K_{ss}^e\right]\end{pmatrix}\begin{Bmatrix}\{d\}\\ \{\phi_a\}\\ \{\phi_s\}\end{Bmatrix}=\begin{Bmatrix}\{F^e\}\\ \{G^e\}\\ \{0\}\end{Bmatrix} \tag{10}$$

Considering a laminate made up of *N* layers with a total thickness of *T*, the elemental mass and transformed stiffness matrices can be written as

Structural mass: $$\left[M_{uu}^e\right]=\int_V \rho\left[N^T\right][N]dV \tag{11}$$

Structural stiffness:

$$\left[K_{uu}{}^e\right]=\frac{2}{T}\int_{-1}^{1}\int_{-1}^{1}\sum_{k=1}^{N}\frac{t_k-t_{k-1}}{2}\int_{-1}^{1}\left[B_u\right]^T[C]\left[B_u\right]|J|d\xi d\eta d\zeta \tag{12}$$

Dielectric conductivity:

$$\left[K_{\phi\phi}{}^e\right]=-\frac{2}{T}\int_{-1}^{1}\int_{-1}^{1}\sum_{k=1}^{N}\frac{t_k-t_{k-1}}{2}\int_{-1}^{1}\left[B_\phi\right]^T[\epsilon]\left[B_\phi\right]|J|d\xi d\eta d\zeta \tag{13}$$

Piezoelectric coupling matrix:

$$\left[K_{u\phi}{}^e\right]=\frac{2}{T}\int_{-1}^{1}\int_{-1}^{1}\sum_{k=1}^{N}\frac{t_k-t_{k-1}}{2}\int_{-1}^{1}\left[B_u\right]^T[e]^T\left[B_\phi\right]|J|d\xi d\eta d\zeta \tag{14}$$

After assembling the elemental stiffness matrices, the global set of equations become

$$\left[M_{uu}\right]\left\{\ddot{d}\right\}+\left[K_{uu}\right]\{d\}+\left[K_{ua}\right]\{\phi_a\}=\{F\} \tag{15}$$

$$\left[K_{au}\right]\{d\}+\left[K_{aa}\right]\{\phi_a\}=\{G\} \tag{16}$$

$$\left[K_{su}\right]\{d\}+\left[K_{ss}\right]\{\phi_s\}=0 \tag{17}$$

For open electrodes, charge can be expressed as

$$\{G\}=0 \tag{18}$$

The overall dynamic finite element equation can be is

$$\left[M_{uu}\right]\left\{\ddot{d}\right\}+\left[[K_{uu}]-[K_{ua}][K_{aa}]^{-1}[K_{au}]-[K_{us}][K_{ss}]^{-1}[K_{su}]\right]\{d\}=\{F\}-\left[K_{ua}\right]\{\phi_a\} \tag{19}$$

where $\left[M_{uu}\right]$ is the global mass matrix, $\left[K_{uu}\right]$ is the global elastic stiffness matrix, $\left[K_{ua}\right]$ and $\left[K_{us}\right]$ are the global piezoelectric coupling matrices of actuator and sensor patches respectively. $\left[K_{aa}\right]$ and $\left[K_{ss}\right]$ are the global dielectric stiffness matrices of actuator and sensor patches respectively. The displacement vector $d(t)$ is approximated by the modal superposition of the first '*r*' modes as

$$\{d(t)\}\approx[\psi]\{\eta(t)\} \tag{20}$$

where $[\psi]=[\psi 1\ \psi 2.....\psi r]$ is the truncated modal matrix.

The decoupled dynamic equations considering modal damping can be written as

$$\left\{\ddot{\eta_i}(t)\right\}+2\xi_{di}\omega_i\left\{\dot{\eta_i}(t)\right\}+\omega_i^2\left\{\eta_i(t)\right\}=\left[\psi\right]^T\{F\}-\left[\psi\right]^T\left[K_{ua}\right]\{\phi_a\} \tag{21}$$

where ξ_{di} is the damping ratio. In state-space form

$$\left\{\dot{X}\right\}=\left[A\right]\{X\}+\left[B\right]\{\phi_a\}+\left[\hat{B}\right]\{u_d\} \tag{22}$$

where, $[A]=\begin{bmatrix}[0] & [I]\\ \left[-\omega_i^2\right] & \left[-2\xi_{di}\omega_i\right]\end{bmatrix}$ is the system matrix, $[B]=\begin{bmatrix}[0]\\ -[\psi]^T\left[K_{ua}\right]\end{bmatrix}$ is the control matrix, $\left[\hat{B}\right]=\begin{bmatrix}[0]\\ [\psi]^T\{F\}\end{bmatrix}$ is the disturbance matrix, $\{u_d\}$ is the disturbance input vector, $\{\phi_a\}$ is the control input, and

$$\left\{\dot{X}\right\}=\begin{Bmatrix}\dot{\eta}\\ \ddot{\eta}\end{Bmatrix}\quad\text{and}\quad\{X\}=\begin{Bmatrix}\eta\\ \dot{\eta}\end{Bmatrix} \tag{23}$$

The sensor output equation can be written as

$$\{y\}=[C_0]\{X\} \tag{24}$$

where output matrix $[C_0]$ depends on the modal matrix $[\psi]$ and the sensor coupling matrix $\left[K_{us}\right]$.

LQR optimal control theory has been used to determine the control gains by minimizing a cost function or a performance index given by

$$J = \frac{1}{2}\int_{t_0}^{t_f} (\{y\}^T[Q]\{y\}+\{\phi_a\}^T[R]\{\phi_a\})dt \quad (25)$$

where *[Q]* and *[R]* are the semi-positive-definite and positive-definite weighting matrices on the outputs and control inputs, respectively.

Minimization of *J* leads to the steady-state matrix Ricatti equation whose solution leads to the gain as

$$\left[G_c\right] = [R]^{-1}[B]^T[K] \quad (26)$$

Considering output feedback, actuation voltage can be calculated as

$$\{\phi_a\} = -[G_c]\{y\} \quad (27)$$

Ang and Quek [2] proposed that [*Q*] and [*R*] matrices could be determined considering weighted energy of the system as follows

$$[Q] = \begin{bmatrix} \alpha_2[\psi]^T[K][\psi] & [0] \\ [0] & \alpha_1[\psi]^T[M][\psi] \end{bmatrix}, \text{and } [R] = \gamma[\hat{R}] \quad (28)$$

The proposed weighted energy of the system in the quadratic form is

$$\bar{\Pi} = \frac{1}{2}\alpha_1\{\dot{X}\}^T[M]\{\dot{X}\} + \frac{1}{2}\alpha_2\{X\}^T[K]\{X\} + \frac{1}{2}\gamma\{\phi_a\}^T[\hat{R}]\{\phi_a\} \quad (29)$$

where, α_1, α_2 and γ are the coefficients associated with total kinetic energy, strain energy and input energy respectively. These coefficients will take different values in the control algorithm apart from the value of unity to allow for the relative importance of these energy terms.

Therefore, a search algorithm is required for finding [*Q*] and [*R*] by taking α_1, α_2 and γ as variables, which will

$$Maximize\ \xi_d = \frac{1}{\sqrt{\left(1+\frac{4\pi^2}{p^2}\right)}} \quad (30)$$

Subjected to $\phi_i < \phi_{max}, i = 1,\ldots n_a$ (31)

where $p = \ln\left(\frac{x_i}{x_{i+1}}\right)$, n_a is the number of actuators and ϕ_{max} refers to the maximum voltage that can be applied on the actuators depending on the piezoelectric materials and thickness of the piezolayers.

3. GA APPROACH TO LQR

In the present work, weighting matrices have been determined by the genetic search to obtain best control gain for the optimal LQR scheme. Parameters α_1, α_2 and γ in Eq. (36) have been represented by real-valued genes for finding [*Q*] and [*R*] matrices. The fitness value has been calculated with respect to each chromosome using the following expression.

$$\xi_d = \begin{cases} \left(\frac{1}{\sqrt{\left(1+\frac{4\pi^2}{p^2}\right)}}\right), & if\ \phi_i < \phi_{max} \\ \left[10^{-8}\times\left(\frac{1}{\sqrt{\left(1+\frac{4\pi^2}{p^2}\right)}}\right)\right], & otherwise \end{cases} \quad (32)$$

The ranges of α_1, α_2 and γ are taken as $0<\alpha_1\leq 200$, $0 < \alpha_2 \leq 200$ and $0 < \gamma \leq 2$ where controlled response depends on α_1, α_2 and γ. Parents have been selected through roulette wheel operator and offspring have been created using simulated binary crossover and polynomial mutation operator [8]. Genetic evolution has been continued for large number of generations till the fitness converges.

4. RESULTS AND DISCUSSIONS

Based on the formulations described in the previous section a code has been developed. The code is first validated with benchmark problems and then applied for simulation of vibration control.

4.1 Validation

A cantilever bimorph (as shown in Fig. 3) made of two PVDF layers laminated together is subjected to a unit external voltage. The transverse deflections calculated have been compared with the already published results of Hwang and Park [14] in the Table 1 and excellent agreements have been achieved.

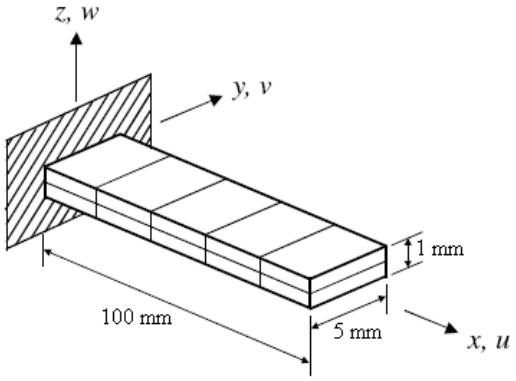

Fig 3. Schematic view of a cantilever bimorph beam.

Table 1: Deflections of piezoelectric bimorph actuator

Distance from fixed end (mm)	**Deflection** (μm)	
	Hwang and Park [14]	**Present FEM**
20	0.0131	0.0136
40	0.0545	0.0540
60	0.1200	0.1223
80	0.2180	0.2181
100	0.3400	0.3416

4.2 Control of an Ellipsoidal Shell Panel

In this study, a simply supported smart graphite/epoxy composite ellipsoidal shell panel on a square base ($a = b$ = 0.04 m) has been considered to study the vibration control. The major axis length is $2\times R$ and minor axis length is $1.5\times R$. The radius is taken as R = 0.06 m. The stacking sequence of each smart graphite/epoxy laminated structure considered is [p/[0/90]$_s$/p]]. Here 'p' stands for piezo-patches one for sensing and the other for actuation. In all the cases, thickness of each piezoelectric patch has been considered as 0.5 mm, the allowable voltage of each PZT patch has been taken as 500V[15]

and thickness of each FRP composite ply has been considered as 0.75 mm. Table 2 shows the material properties considered in the present study.

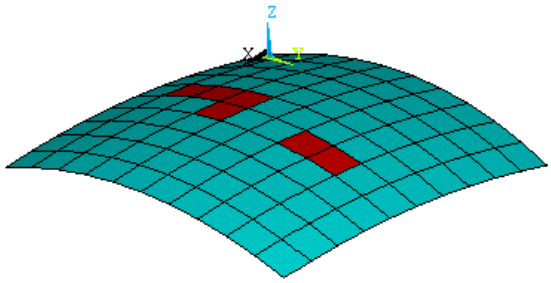

Fig 4. Collocated sensors and actuators location

Six numbers of collocated sensors and actuators have been considered and based on an optimal placement scheme those are placed as shown in figure 4. A modal damping ratio (ξ_d) of 1% has been assumed to obtain open loop response and to calculate LQR gains. The smart panel has been subjected to an impulse load of 10 N at the center for a duration of $\tau/25$ seconds (where τ is the time period corresponding to first natural frequency of the system) and impulse responses of this panel have been calculated with a time step of $\tau/100$ seconds.

Table 2: Material Properties

Material properties	**Structural laminae**	**PZT**
E_1	172.5 GPa	63.0 GPa
$E_2 = E_3$	6.9 GPa	63.0 GPa
$G_{12} = G_{13}$	3.45 GPa	24.6 GPa
G_{23}	1.38 GPa	24.6 GPa
$\upsilon_{12} = \upsilon_{13} = \upsilon_{23}$	0.25	0.28
ρ	1600 kg m^{-3}	7600 kg m^{-3}
$e_{31} = e_{32}$	0.0	10.62 C m^{-2}
$\in_{11} = \in_{22} = \in_{33}$	0.0	0.1555x10^{-7}F m^{-1}

Uncontrolled displacement of the ellipsoidal shell panel is shown in Fig.5. The LQR and GA-LQR controlled displacement histories of smart ellipsoidal panel have been depicted in Fig. 6. It could be observed from figure 6 that both simple LQR and GA-LQR could control the vibration. However, in the GA-LQR controlled response of the panel, the closed loop-damping ratio achieved has been 17% compared to only 3.12% in the case of simple LQR control scheme. The maximum actuator voltage variations for simple LQR and GA-LQR control scheme have been shown in Fig. 7, which clearly shows that the GA-LQR control scheme could achieve, better control with minimum actuation voltage requirement. From this study it could be concluded that GA-LQR control scheme leads to the maximization of closed loop damping ratio with minimum input/actuator voltage within the limit.

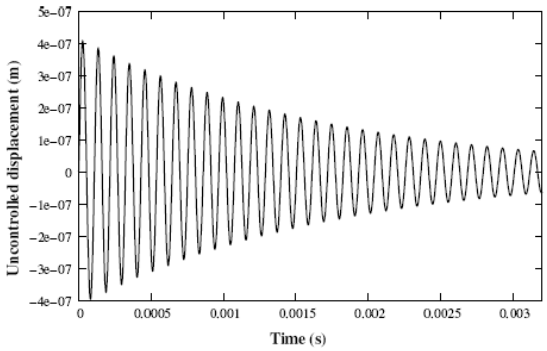

Fig 5. Uncontrolled displacement history

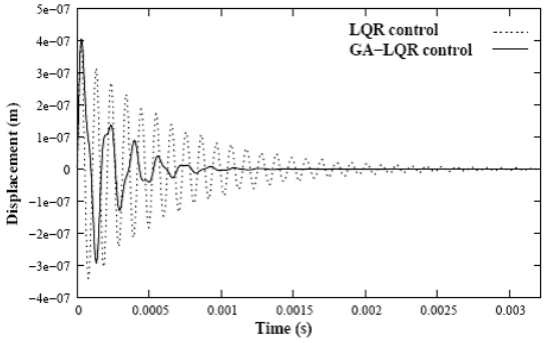

Fig 6. LQR and GA-LQR controlled displacements

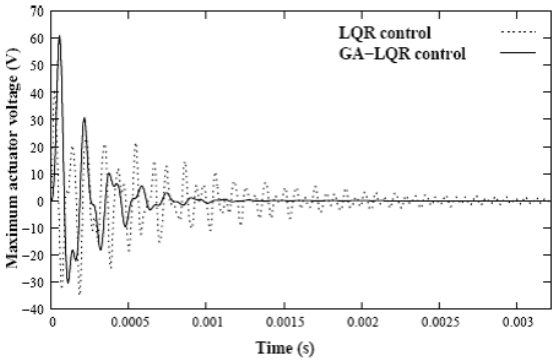

Fig 7. Maximum actuator voltage variation using LQR and GA-LQR control schemes

5. CONCLUSIONS

In the present work, a GA based LQR optimal control scheme have been developed for optimal vibration control of smart shell structures. This module along with layered shell finite element analysis has been used to simulate active vibration control of smart ellipsoidal shell FRP structures. It has been observed that the present GA based LQR scheme is far superior to conventional LQR scheme in terms of effective closed loop damping ratio and minimizing the actuator voltage requirement while keeping it within limit. Therefore this could be advantageously used in design of control gains in smart structures applications.

6. REFERENCES

1. Bhattacharya, P., Suhail, H. and Sinha, P. K., 2002, “Finite Element Analysis and Distributed Control of Laminated Composite Shells using LQR/IMSC Approach”, Aerospace Science and Technology, 6:273–281.
2. Ang, K .K., Wang, S.Y. and Quek S. T., 2002, “Weighted Energy Linear Quadratic Regulator Vibration Control of Piezoelectric Composite Plates”, Journal of Smart Materials and Structures, 11:98-106.
3. Narayanan, S. and Balamurugan, V., 2003, “Finite Element Modeling of Piezolaminated Smart Structures for Active Vibration Control with Distributed Sensors and Actuators”, Journal of Sound and Vibration, 262:529–562.
4. Han, J.H. and Lee, L., 1999, “Optimal Placement of Piezoelectric Sensors and Actuators for Vibration Control of a Composite Plate using Genetic Algorithms”, Journal of Smart Materials and Structures, 8:257-267.
5. Sadri, A.M., Wright, J.R., and Wynne, R, 1999, “Modeling and Optimal Placement of Piezoelectric Actuators in Isotropic Plates using Genetic Algorithm”, Journal of Smart Materials and Structures, 8:490-498.
6. Abdullah, M. M., Richardson, A. and Hanif, J. 2001, “Placement of Sensors/Actuators on Civil Structures using Genetic Algorithms”, Earthquake Engineering & Structural Dynamics, 30 (8):1167-1184.
7. Robandi, I., Nishimori, K., Nishimura, R. and Ishihara N., 2001, “Optimal Feedback Control Design using Genetic Algorithm in Multimachine Power system”, Electrical Power and Energy Systems, 23:263-271.
8. Deb, K. and Gulati, S., 2001, “Design of Truss-Structures for Minimum Weight Using Genetic Algorithms”, Finite Elements in Analysis and Design, 37:447-465.
9. Yang, Y., Jin, Z. and Soh, C.K., 2005, “Integrated Optimal Design of Vibration Control System for Smart Beams using Genetic Algorithm”, Journal of Sound and Vibration, 282:1293-1307.
10. Wang, S.Y., Tai, K. and Quek, S.T., 2006, “Topology Optimization of Piezoelectric Sensors/Actuators for Torsional Vibration Control of Composite Plates”, Journal of Smart Materials and structures, 15(2):253-269
11. Liu, W., Hou, Z.K. and Demetriou, M.A., 2006, “A Computational Scheme for the Optimal Sensor/Actuator Placement of Flexible Structures using Spatial H-2 Measures”, Mechanical Systems and Signal Processing, 20 (4):881-895.
12. Swann, C. and Chattopadhyay, A., 2006, “Optimization of Piezoelectric Sensor Location for Delamination Detection in Composite Laminates”, Engineering Optimization, 38 (5):511-528.
13. Ahamad, S., Irons, B.M. and Zienkiewicz, O. C., 1970, “Analysis of Thick and Thin Shell Structure by Curved Elements”, Int. J. Numer Meth Engg, 2:419-451.
14. Hwang, W. S. and Park, H. C. 1993, “Finite Element Modeling of Piezoelectric Sensors and Actuators”, AIAA Journal, 31 (5):930-937.
15. Bruch, J.C., Sloss, J.M. and Sadek, I. S., 2002, “Optimal Piezo-Actuator Locations/Lengths and Applied Voltage for Shape Control of Beams”, Journal of Smart Materials and Structures, 9:205-211.

7. ACKNOWLEDGEMENT

The authors gratefully acknowledge the support of the SERC (Grant No. SR/S3/MERC/0017/2008) of the Department of Science and Technology, Government of India.

8. MAILING ADDRESS

Prof. Debabrata Chakraborty
Mechanical Engineering,
IIT Guwahati, Guwahati 781 039, India
E-mail: chakra@iitg.ernet.in